Resource

Cell Host & Microbe

A Mouse Model of Zika Virus Pathogenesis

Graphical Abstract

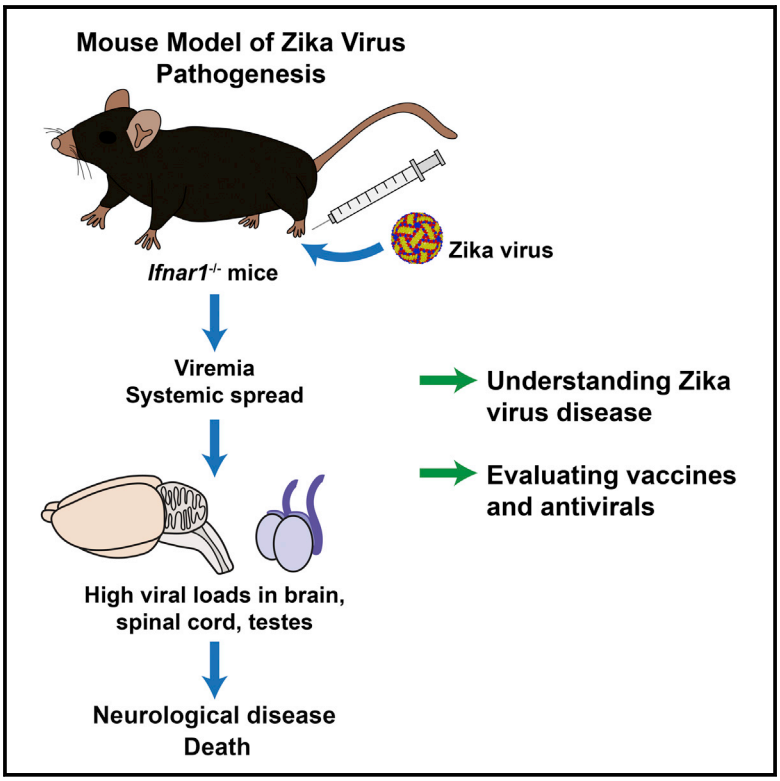

Authors

Helen M. Lazear, Jennifer Govero, Amber M. Smith, Derek J. Platt, Estefania Fernandez, Jonathan J. Miner, Michael S. Diamond

Correspondence

diamond@borcim.wustl.edu

In Brief

The Zika virus epidemic has brought an urgent need for animal models. Lazear et al. describe a mouse model for Zika virus. Mice lacking interferon α/β signaling develop neurological disease and succumb to infection with high viral loads in the brain, spinal cord, and testes, consistent with severe manifestations of Zika virus in humans.

Highlights

- Development of a mouse model of ZIKV pathogenesis including multiple viral strains
- *Ifnar1*$^{-/-}$ mice sustain high viral burden in brain, spinal cord, and testes
- ZIKV can establish viremia in the absence of clinical signs in mice
- ZIKV mouse model may be useful for vaccine and antiviral testing

Lazear et al., 2016, Cell Host & Microbe *19*, 720–730
May 11, 2016
http://dx.doi.org/10.1016/j.chom.2016.03.010

CellPress

Cell Host & Microbe
Resource

A Mouse Model of Zika Virus Pathogenesis

Helen M. Lazear,[1] Jennifer Govero,[2] Amber M. Smith,[2] Derek J. Platt,[2] Estefania Fernandez,[2] Jonathan J. Miner,[2] and Michael S. Diamond[2,3,4,5,*]

[1]Department of Microbiology and Immunology, University of North Carolina at Chapel Hill, Chapel Hill, NC 27599, USA
[2]Department of Medicine
[3]Department of Molecular Microbiology
[4]Department of Pathology & Immunology
[5]The Center for Human Immunology and Immunotherapy Programs
Washington University School of Medicine, St. Louis, MO 63110, USA
*Correspondence: diamond@borcim.wustl.edu
http://dx.doi.org/10.1016/j.chom.2016.03.010

SUMMARY

The ongoing Zika virus (ZIKV) epidemic and unexpected clinical outcomes, including Guillain-Barré syndrome and birth defects, has brought an urgent need for animal models. We evaluated infection and pathogenesis with contemporary and historical ZIKV strains in immunocompetent mice and mice lacking components of the antiviral response. Four- to six-week-old *Irf3*$^{-/-}$ *Irf5*$^{-/-}$ *Irf7*$^{-/-}$ triple knockout mice, which produce little interferon α/β, and mice lacking the interferon receptor (*Ifnar1*$^{-/-}$) developed neurological disease and succumbed to ZIKV infection, whereas single *Irf3*$^{-/-}$, *Irf5*$^{-/-}$, and *Mavs*$^{-/-}$ knockout mice exhibited no overt illness. *Ifnar1*$^{-/-}$ mice sustained high viral loads in the brain and spinal cord, consistent with evidence that ZIKV causes neurodevelopmental defects in human fetuses. The testes of *Ifnar1*$^{-/-}$ mice had the highest viral loads, which is relevant to sexual transmission of ZIKV. This model of ZIKV pathogenesis will be valuable for evaluating vaccines and therapeutics as well as understanding disease pathogenesis.

INTRODUCTION

Zika virus (ZIKV) belongs to the Flavivirus genus of the *Flaviviridae* family, which includes globally relevant arthropod-transmitted human pathogens such as dengue (DENV), yellow fever (YFV), West Nile (WNV), Japanese encephalitis (JEV), and tick-borne encephalitis viruses (Lazear and Diamond, 2016; Pierson and Diamond, 2013). Within the mosquito-borne clade of flaviviruses, ZIKV is a member of the Spondweni group; both genetically and serologically, ZIKV is related closely to the four serotypes of DENV with approximately 43% amino acid identity and extensive antibody cross-reactivity (Alkan et al., 2015; Lanciotti et al., 2008).

The first strain of ZIKV (MR 766) was isolated in 1947 from a febrile sentinel rhesus monkey in the Zika forest near Entebbe, Uganda after intracerebral passage in Swiss albino mice (Dick, 1952; Dick et al., 1952). In the decades following its discovery, ZIKV was isolated from human patients sporadically during outbreaks in Africa and Southeast Asia (Haddow et al., 2012; Hayes, 2009), but remained obscure due to the fairly benign nature of the infection (Lazear and Diamond, 2016). Typically, ZIKV infection has been associated with a self-limiting febrile illness often including rash, arthralgia, and conjunctivitis, though most infections are asymptomatic (Brasil et al., 2016; Duffy et al., 2009; Hayes, 2009). Despite the mild disease historically associated with ZIKV infection, more severe complications have been noted during recent outbreaks in the South Pacific and Latin America.

The first association between ZIKV infection and neurological disorders occurred during the 2013–2014 ZIKV outbreak in French Polynesia (Cao-Lormeau et al., 2014), which was associated with a 20-fold increase in cases of Guillain-Barré syndrome (GBS) (Cao-Lormeau et al., 2016; Oehler et al., 2014). GBS is a post-infection autoimmune peripheral neuropathy that can produce pain, weakness, and paralysis; although GBS usually is temporary, GBS-induced respiratory paralysis can be fatal (Willison et al., 2016). In support of a causal link between ZIKV and GBS, the emergence of ZIKV in the western hemisphere in 2015–2016 has been associated temporally with increased numbers of GBS cases in Brazil, El Salvador, and Colombia (European Centre for Disease Prevention and Control, 2016).

During the current epidemic in Latin America, ZIKV infection has been linked to the development of severe fetal abnormalities that include spontaneous abortion, stillbirth, hydranencephaly, microcephaly, and placental insufficiency that may cause intrauterine growth restriction (Brasil et al., 2016; Sarno et al., 2016; Ventura et al., 2016). Furthermore, a retrospective analysis identified an increase in microcephaly cases during the 2013–2014 ZIKV outbreak in French Polynesia (Cauchemez et al., 2016). Several cases of presumed intrauterine ZIKV infection resulted in coarse cerebral calcifications in different brain regions of newborn infants or fetuses in utero (Oliveira Melo et al., 2016). The reported congenital malformation cases may represent only the most severe end of the spectrum, with less severe infection producing long-term cognitive or functional sequelae. Indeed, ocular findings in infants with presumed ZIKV-associated microcephaly were reported recently (de Paula Freitas et al., 2016). While much remains to be determined about the mechanisms by which ZIKV mediates microcephaly and other birth defects, mounting molecular and immunologic evidence supports the conclusion that ZIKV can cross the placenta and damage a developing fetus. This evidence includes detection

of ZIKV RNA, full-length viral genome, or viral particles in the amniotic fluid or brains of fetuses diagnosed with microcephaly, as well as ZIKV IgM in amniotic fluid, consistent with fetal infection (Calvet et al., 2016; Martines et al., 2016; Mlakar et al., 2016; Oliveira Melo et al., 2016; Petersen et al., 2016).

Little is known about the cellular and tissue tropism of ZIKV, but keratinocytes and dendritic cells in the skin likely represent early targets of infection, similar to other flaviviruses (Hamel et al., 2015; Lim et al., 2011; Limon-Flores et al., 2005; Surasombatpattana et al., 2011), and ZIKV can infect human skin explants and peripheral blood mononuclear cells in culture (Hamel et al., 2015). Evidence from infants and fetuses infected in utero suggests ZIKV may be neurotropic (Mlakar et al., 2016; Sarno et al., 2016), and a recent report demonstrated ZIKV infection in human neuroprogenitor cells in culture (Tang et al., 2016).

Vaccines and therapeutics are needed urgently to combat ZIKV, and testing would be expedited by animal models of the different manifestations of disease. Multiple monkey species in the Zika forest were found to be seropositive for ZIKV (McCrae and Kirya, 1982), suggesting they can become infected and support viral replication. Other mammals in the Zika forest (including squirrels, tree rats, giant pouched rats, and civets) did not show serological evidence of ZIKV infection (Haddow et al., 1964), though a subsequent study in Kenya detected ZIKV antibodies in small mammals including rats and shrews (Johnson et al., 1977). In response to the ongoing epidemic, new ZIKV studies have been initiated in animals including rhesus macaques (https://zika.labkey.com/project/OConnor/ZIKV-001/begin.view).

Until very recently, few studies had been performed in mice (Bell et al., 1971; Dick, 1952; Way et al., 1976). Although these early studies suggested that ZIKV can replicate and cause injury in cells of the central nervous system (CNS), it is uncertain whether this pathogenesis is related to ZIKV-induced neurodevelopmental defects or GBS in humans. Moreover, these studies used the prototype MR 766 strain of ZIKV, which had undergone extensive passage in suckling mouse brains, and to date no experiments have been reported in mice with more contemporary ZIKV isolates of greater clinical relevance. To address this fundamental gap in knowledge, we evaluated ZIKV infection and disease in wild-type (WT) C57BL/6 mice, as well as a large panel of immune-deficient transgenic mice, using several strains of ZIKV including a contemporary clinical isolate. Whereas 4- to 6-week-old WT mice did not develop clinically apparent disease, mice lacking interferon α/β (IFN-α/β) signaling (i.e., *Ifnar1*$^{-/-}$ or *Irf3*$^{-/-}$ *Irf5*$^{-/-}$ *Irf7*$^{-/-}$ triple knockout [TKO] mice) succumbed to infection with different ZIKV strains. Viral burden analysis revealed that *Ifnar1*$^{-/-}$ but not WT mice sustained high levels of ZIKV in all tissues tested, including serum, spleen, brain, spinal cord, and testes. Our studies establish a mouse model of ZIKV pathogenesis with contemporary and historical virus strains that will be valuable for evaluating candidate vaccines and therapeutics as well as understanding the basic biology of ZIKV infection and disease.

RESULTS

Susceptibility of Immunocompetent and Immunodeficient Mice to ZIKV

Small animal models of ZIKV pathogenesis are a key research priority in response to the ZIKV epidemic in Latin America and the Caribbean. Historical studies indicated that mice could be infected with ZIKV via intracerebral inoculation, but determining mechanisms of pathogenesis and evaluating candidate antivirals and vaccines requires more clinically relevant inoculation routes and validation with contemporary ZIKV strains. We tested 5- to 6-week-old WT C57BL/6 mice as well as congenic transgenic mice lacking key components of innate antiviral immunity (*Ifnar1*$^{-/-}$, *Mavs*$^{-/-}$, *Irf3*$^{-/-}$, *Irf3*$^{-/-}$ *Irf5*$^{-/-}$ *Irf7*$^{-/-}$ TKO) for susceptibility to disease induced by a contemporary human isolate of ZIKV (H/PF/2013) from French Polynesia, as well as the original ZIKV strain, MR 766 (Figures 1A–1D). *Ifnar1*$^{-/-}$ mice (which cannot respond to IFN-α/β) and *Irf3*$^{-/-}$ *Irf5*$^{-/-}$ *Irf7*$^{-/-}$ TKO mice (which produce almost no IFN-α/β) (Lazear et al., 2013) were highly vulnerable to ZIKV infection. Both strains of mice began to lose weight by 5 days after infection, and by day 7, when they began to succumb to infection, they had lost between 15% and 25% of their starting body weight. *Ifnar1*$^{-/-}$ and *Irf3*$^{-/-}$ *Irf5*$^{-/-}$ *Irf7*$^{-/-}$ TKO mice both exhibited 100% lethality by 10 days after infection with ZIKV (H/PF/2013). *Ifnar1*$^{-/-}$ and *Irf3*$^{-/-}$ *Irf5*$^{-/-}$ *Irf7*$^{-/-}$ TKO mice all developed neurological disease signs including hindlimb weakness and paralysis before succumbing to the infection (Figures 2A and 2B). In comparison, WT mice or those lacking the signaling adaptor MAVS or the transcription factor IRF-3 (both of which play key roles in IFN-α/β induction) exhibited no weight loss, morbidity, or mortality. We saw a similar pattern of ZIKV susceptibility when WT, *Ifnar1*$^{-/-}$, and *Irf3*$^{-/-}$ *Irf5*$^{-/-}$ *Irf7*$^{-/-}$ TKO mice were infected via an intravenous route, rather than a subcutaneous one (Figures 1E and 1F and Figure 2C).

Irf3$^{-/-}$ *Irf5*$^{-/-}$ *Irf7*$^{-/-}$ TKO mice were more susceptible to ZIKV infection than *Ifnar1*$^{-/-}$ mice following intravenous inoculation ($p < 0.05$ for H/PF/2013, $p < 0.001$ for MR 766), which suggests a possible role for IRF-3-dependent, IFN-α/β-independent restriction mechanisms (Lazear et al., 2013). ZIKV H/PF/2013 was more pathogenic than the original Ugandan strain, as 20% or 60% of *Ifnar1*$^{-/-}$ mice survived infection with MR 766 (by subcutaneous or intravenous inoculation, respectively) compared to 100% lethality after H/PF/2013 infection ($p < 0.001$ for subcutaneous, $p < 0.0001$ for intravenous).

Although *Ifnar1*$^{-/-}$ and *Irf3*$^{-/-}$ *Irf5*$^{-/-}$ *Irf7*$^{-/-}$ TKO mice can be used as models to evaluate, for example, activity of candidate antivirals against ZIKV in vivo, there are limitations to pathogenesis studies in mice lacking a critical component of innate antiviral immunity. We selected three additional ZIKV strains for further characterization and corroboration: Dakar 41671, 41667, and 41519. These viruses were isolated in the 1980s from mosquitoes in the same area of Senegal. We evaluated different infection conditions (i.e., viral strain, inoculation route, mouse age, or mouse genotype) with the goal of identifying a more immunocompetent mouse system that was susceptible to ZIKV disease (Table 1). None of these conditions resulted in lethal ZIKV disease in an adult mouse, though larger group sizes would be necessary to detect infrequent disease presentations. In addition to WT and *Ifnar1*$^{-/-}$ mice, we evaluated infection in CD-1 mice (an outbred mouse line) and *Irf5*$^{-/-}$ mice, infecting 4-week-old mice with 10^3 focus-forming units (FFU) of each of the ZIKV strains from Senegal. Whereas *Ifnar1*$^{-/-}$ mice lost weight rapidly and succumbed to the infection within 1 week, we observed no weight loss or mortality in WT, CD-1,

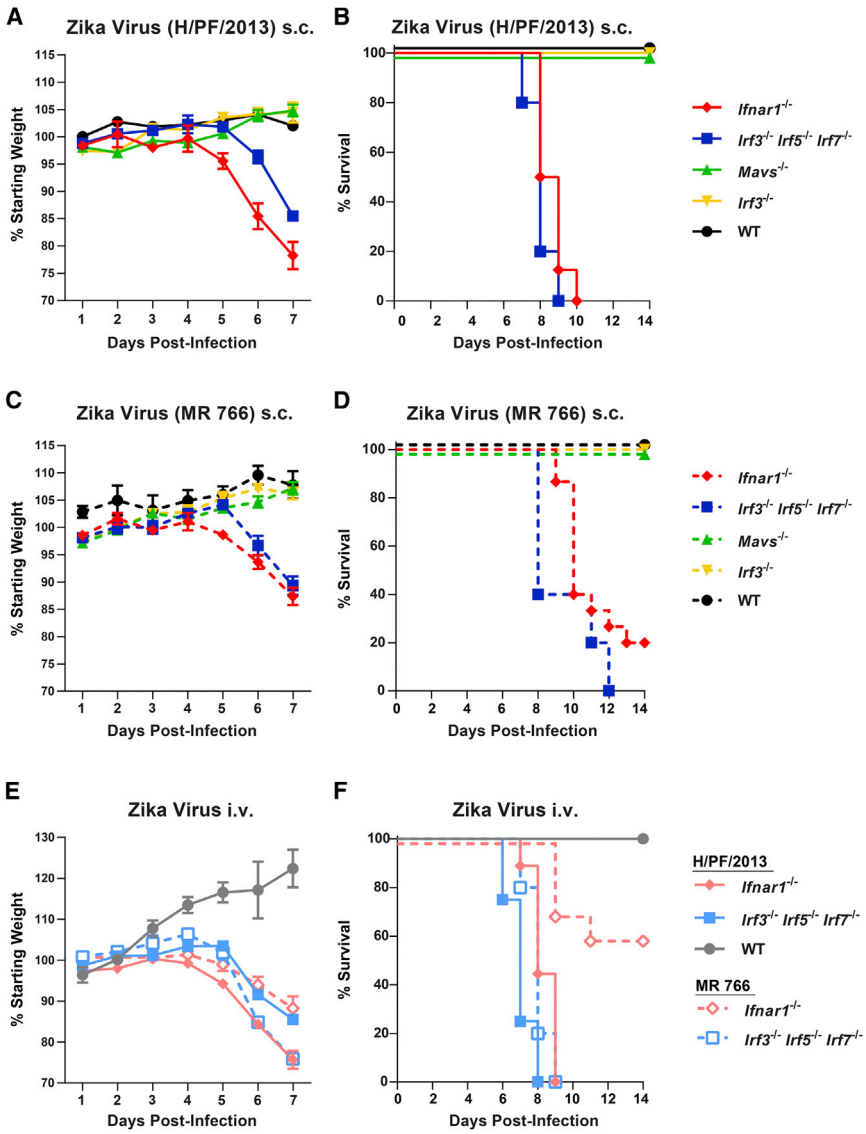

Figure 1. Mice Lacking IFN-α/β Responses Are Susceptible to ZIKV Disease

(A–F) Five- to six-week-old mice of the indicated genotypes were inoculated with 10^2 FFU of ZIKV strain H/PF/2013 or MR 766 by a subcutaneous route (s.c.) in the footpad (A–D) or by an intravenous (i.v.) route (E and F). Mice were weighed daily and weights are expressed as percentage of body weight prior to infection (A, C, and E). Results shown are the mean ± standard error of the mean (SEM) of the indicated number of mice per group. Data are censored at 7 days after infection, as mice in some groups died. Lethality was monitored for 14 days (B, D, and F). For (A) and (B): n = 16 (*Ifnar1*$^{-/-}$), 5 (*Irf3*$^{-/-}$ *Irf5*$^{-/-}$ *Irf7*$^{-/-}$ TKO, *Mavs*$^{-/-}$, WT), 9 (*Irf3*$^{-/-}$). For (C) and (D): n = 15 (*Ifnar1*$^{-/-}$), 5 (*Irf3*$^{-/-}$ *Irf5*$^{-/-}$ *Irf7*$^{-/-}$ TKO, *Mavs*$^{-/-}$), 9 (*Irf3*$^{-/-}$), 3 (WT). For (E) and (F): n = 9 (*Ifnar1*$^{-/-}$ H/PF/2013), 4 (*Irf3*$^{-/-}$ *Irf5*$^{-/-}$ *Irf7*$^{-/-}$ TKO, WT H/PF/2013), 10 (*Ifnar1*$^{-/-}$ MR 766), 5 (*Irf3*$^{-/-}$ *Irf5*$^{-/-}$ *Irf7*$^{-/-}$ TKO MR 766).

Since IFN-α/β signaling appears to have a key role in restricting ZIKV infection in mice, we tested whether treatment with an IFNAR1-blocking monoclonal antibody (MAR1-5A3) (Sheehan et al., 2006) could render WT mice susceptible to ZIKV disease. This strategy might be valuable for vaccine studies, as it would allow immune responses to be elicited in immunocompetent mice with the possibility of enhancing infection at the time of viral challenge. In prior studies with WNV, a related neurotropic flavivirus, we showed that blockade of IFN-α/β signaling with MAR1-5A3 could recapitulate the susceptible phenotype of *Ifnar1*$^{-/-}$ mice (Pinto et al., 2011; Sheehan et al., 2015). With the goal of establishing a higher-throughput mouse model of ZIKV infection and disease in the context of WT mice, we treated WT mice with 750 μg, 1 mg, or 2 mg of MAR1-5A3 or 2 mg of isotype control antibody via intraperitoneal (i.p.) injection 1 day prior to (as well as after, for the 2 mg total dose) infection with 10^3 FFU of ZIKV (H/PF/2013) (Figure 5). Although mice did not lose weight or succumb to infection, animals treated with 1 or 2 mg of MAR1-5A3 developed higher viral loads at day 3 after infection compared to control treated mice. This model may be useful for evaluating protection elicited by candidate ZIKV vaccines, using viremia as a correlate of protection rather than morbidity or mortality. These observations also demonstrate that ZIKV can replicate and establish viremia even in the absence of clinical disease signs.

or *Irf5*$^{-/-}$ mice (Figures 3A–3C). However, when we infected suckling WT mice (1 week old), we observed susceptibility to infection, with 5 of 15 mice succumbing within 24 days (Figure 3D). Taken together, these data suggest that although ZIKV can cause disease in WT mice, it does so in an age-dependent manner and likely is inefficient in the context of a robust innate immune response.

We performed additional experiments to characterize ZIKV infection in older *Ifnar1*$^{-/-}$ mice to determine the possible utility of the model for vaccine studies. Whereas 4- to 6-week-old *Ifnar1*$^{-/-}$ mice succumb to infection by several strains of ZIKV, vaccine studies will require mice to be older at the time of viral challenge due to the timing of prime-boost regimens. To test whether older *Ifnar1*$^{-/-}$ mice remain vulnerable to ZIKV infection, we infected 3-, 4-, and 6-month-old *Ifnar1*$^{-/-}$ mice with 10^3 FFU of ZIKV (H/PF/2013) and monitored weight loss and lethality (Figure 4). Mice of all ages lost weight after ZIKV infection, with ~30% of starting weight lost by 9 days after infection. Despite the significant weight loss, 40%–80% of mice ultimately survived infection.

Tissue Tropism of ZIKV in Mice

We next determined the tissue tropism of ZIKV by infecting 4- to 6-week-old WT and *Ifnar1*$^{-/-}$ mice with 10^3 FFU of ZIKV (H/PF/2013) by subcutaneous inoculation and measuring viral burden in tissues at 2 or 6 days after infection (Figure 6). ZIKV replicated

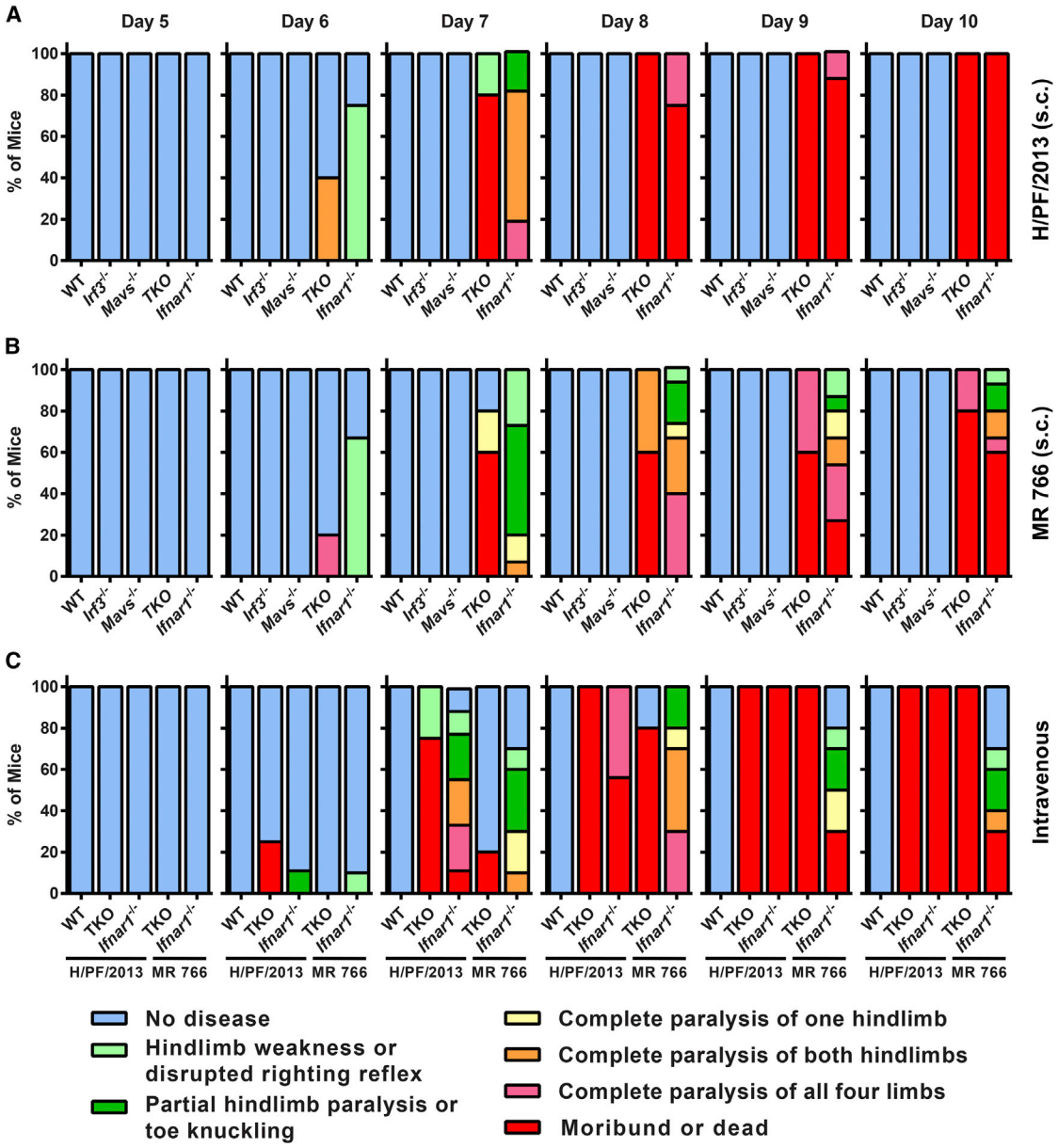

Figure 2. ZIKV Infection Produces Neurologic Disease in *Ifnar1*$^{-/-}$ and *Irf3*$^{-/-}$ *Irf5*$^{-/-}$ *Irf7*$^{-/-}$ TKO Mice

(A–C) Mice of the indicated genotypes were infected with ZIKV strain H/PF/2013 (A) or MR 766 (B) by a subcutaneous (s.c.) (A and B) or intravenous (C) route, and disease signs were assessed daily for 10 days. The percentage of each group of mice displaying the indicated signs is shown. These are the same mice evaluated for weight loss and lethality in Figure 1.

inefficiently in WT mice, with levels of viral RNA above background observed primarily in the spleen (Figures 6A–6G). In comparison, *Ifnar1*$^{-/-}$ mice sustained higher viral loads in all tested tissues (spleen, liver, kidney, serum, testes, brain, and spinal cord). By 6 days after infection, high levels of ZIKV viral RNA were observed in CNS tissues of *Ifnar1*$^{-/-}$ mice (> 10^6 FFU equivalents per gram in the brain and spinal cord), confirming the neurotropic potential of the virus (Bell et al., 1971; Martines et al., 2016; Mlakar et al., 2016; Sarno et al., 2016; Tang et al., 2016). Remarkably, the highest levels of ZIKV RNA (10^7 FFU equivalents per gram) were present in the testes, which could explain male-to-female sexual transmission of ZIKV observed in humans (Foy et al., 2011; Hills et al., 2016; Musso et al., 2015; Venturi et al., 2016). We performed plaque assays to measure infectious ZIKV in the testes, brain, and spinal cord. Consistent with the qRT-PCR results, we found high levels of ZIKV in all three tissues in *Ifnar1*$^{-/-}$ mice at 6 days after infection (Figures 6I–6K). To determine whether ZIKV can persist in tissues after clinical disease signs have resolved, we measured viral RNA levels in the brain and testes 28 days after ZIKV H/PF/2013 infection from surviving 3-, 4-, or 6-month-old *Ifnar1*$^{-/-}$ mice. ZIKV RNA was detected in all surviving animals, with approximately

Table 1. ZIKV Infection in Different Strains of Mice

Mouse	Age (weeks)	ZIKV Strain (Dakar)	Dose (FFU)	Route	Number infected	Survival (%)
WT	4	41519	1×10^3	s.c.	5	100
WT	4	41667	1×10^3	s.c.	5	100
WT	4	41671	1×10^3	s.c.	5	100
WT	1	41519	1×10^4	i.p.	15	67
CD-1	4	41519	1×10^3	s.c.	5	100
CD-1	4	41667	1×10^3	s.c.	5	100
CD-1	4	41671	1×10^3	s.c.	5	100
AG129	4	41519	1×10^4	s.c.	5	0
Ifnar1$^{-/-}$	4	41519	1×10^3	s.c.	3	0
Ifnar1$^{-/-}$	4	41667	1×10^3	s.c.	2	0
Ifnar1$^{-/-}$	4	41671	1×10^3	s.c.	2	0
Mavs$^{-/-}$	7	41519	1×10^4	s.c.	8	100
Ifnlr1$^{-/-}$	4	41519	1×10^4	s.c.	5	100
Irf3$^{-/-}$	8	41519	1×10^4	i.p.	4	100
Irf3$^{-/-}$	8	41519	1×10^4	s.c.	4	100
Irf5$^{-/-}$	4	41519	1×10^4	i.p.	5	100
Irf5$^{-/-}$	4	41519	5×10^4	i.p.	2	100
Irf5$^{-/-}$	4	41519	1×10^4	s.c.	8	100
Irf5$^{-/-}$	4	41519	1×10^3	s.c.	5	100
Irf5$^{-/-}$	4	41667	1×10^3	s.c.	5	100
Irf5$^{-/-}$	4	41671	1×10^3	s.c.	5	100
Ifit1$^{-/-}$	4	41519	1×10^4	s.c.	5	100
Ifit2$^{-/-}$	4	41519	1×10^4	s.c.	5	100
Ifitm3$^{-/-}$	4	41519	1×10^4	s.c.	3	100
Isg15$^{-/-}$	4	41519	1×10^4	s.c.	4	100
Isg15$^{-/-}$	6	41519	1×10^4	s.c.	10	100
Ube1l$^{-/-}$	4	41519	1×10^4	s.c.	5	100
Mb21d1$^{-/-}$ (cGas)	4	41519	1×10^4	s.c.	5	100
Mb21d1$^{-/-}$ x *Tmem173*$^{-/-}$ DKO	4	41519	1×10^4	s.c.	3	100
Tmem173$^{-/-}$ (STING)	4	41519	1×10^4	s.c.	5	100

s.c., subcutaneous route of inoculation; i.p., intraperitoneal route of inoculation.

10^4 and 10^5 FFU equivalents per gram in the brain and testes, respectively. In the brain, the age at the time of infection did not impact the level of viral RNA persistence. As only two male mice were available for testes analysis (both 4 months old at infection), analogous conclusions could not be established.

DISCUSSION

The emergence of ZIKV in the western hemisphere and in particular the unexpected association between ZIKV, birth defects, and GBS has focused international public health attention on this previously obscure virus and spurred calls for rapid development of vaccines and therapeutics. However, it will be difficult to evaluate candidate products rapidly without small animal models of disease. Furthermore, a mechanistic understanding of ZIKV pathogenesis, which can be determined using animal models of disease, can provide insight into the dynamics of ZIKV spread and transmission.

In our experiments, ZIKV infection did not cause disease in weaned WT mice (> 3 weeks old), results that are consistent with the original description of the prototype ZIKV strain, MR 766, almost 70 years ago. In comparison, suckling WT mice (1 week old) were susceptible to infection. ZIKV replicated and caused disease in juvenile and adult mice lacking IFN-α/β immunity, with spread to many tissues including the CNS and the testes. We observed similar patterns of susceptibility using five different strains of ZIKV, including a contemporary human clinical isolate as well as historical African strains, highlighting the utility of the *Ifnar1*$^{-/-}$ mouse model for a range of studies of ZIKV pathogenesis. Although further studies are warranted, the relative resistance of adult mice may reflect an inability of ZIKV to antagonize murine IFN-α/β signaling or effector functions efficiently, analogous to DENV (Pagni and Fernandez-Sesma, 2012; Suthar et al., 2013). The only adult mice we found susceptible to lethal ZIKV infection were *Ifnar1*$^{-/-}$, *Irf3*$^{-/-}$ *Irf5*$^{-/-}$ *Irf7*$^{-/-}$ TKO, and AG129 (*Ifnar1* and *Ifngr1* deficient) mice, all of which lack the capacity either to respond to or induce IFN-α/β.

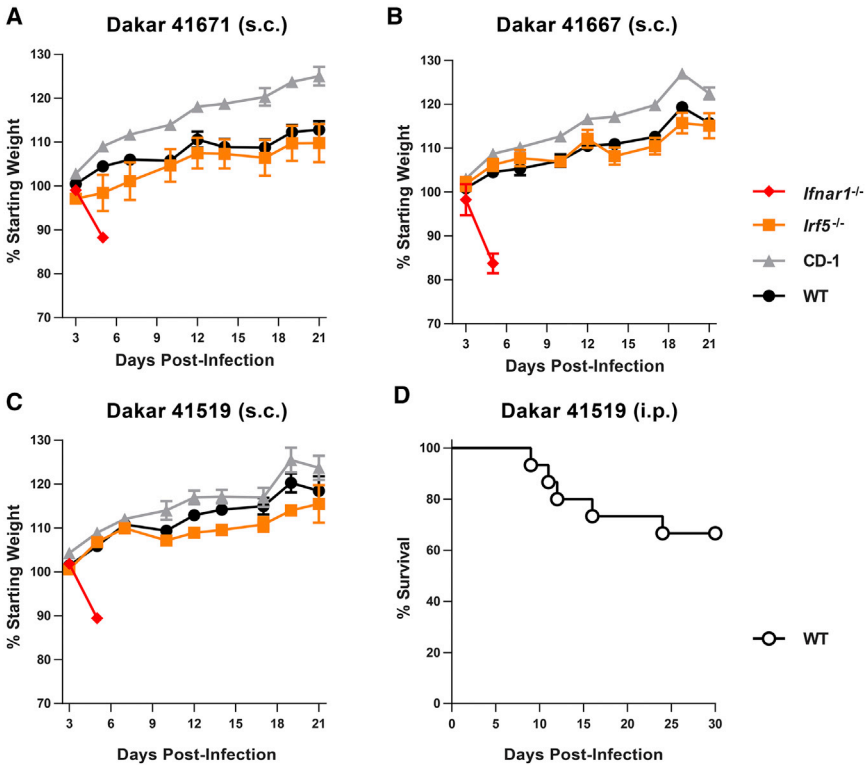

Figure 3. ZIKV Strains from Senegal Cause Lethal Disease in 4-Week-Old *Ifnar1*$^{-/-}$ Mice and 1-Week-Old WT Mice

(A–C) Four-week-old WT (C57BL/6), CD-1, *Irf5*$^{-/-}$, and *Ifnar1*$^{-/-}$ mice were infected with 10^3 FFU of one of three ZIKV strains isolated from mosquitoes in Senegal (Dakar 41671, 41667, or 41519) by a subcutaneous route (s.c.). Weights were obtained over 21 days and are expressed as a percentage of starting weight. *Ifnar1*$^{-/-}$ mice succumbed to the infection after 6 days. Results shown are the mean ± SEM of 4–5 mice per group (WT, CD-1, and *Irf5*$^{-/-}$) or 2–3 mice per group (*Ifnar1*$^{-/-}$).

(D) One-week-old WT mice (n = 15) were infected with 10^4 FFU of ZIKV Dakar 41519 by intraperitoneal (i.p.) injection, and lethality was monitored for 30 days.

Ifnar1$^{-/-}$ mice remained susceptible to ZIKV-induced morbidity and mortality even when infected at 6 months of age, indicating the utility of this model for vaccine challenge studies.

Ifnar1$^{-/-}$ mice have been used previously as a small-animal model for flavivirus pathogenesis, including for DENV and YFV (Meier et al., 2009; Pinto et al., 2015; Sarathy et al., 2015; Zellweger et al., 2015). However, we acknowledge the limitations of this mouse model with respect to providing a complete understanding of ZIKV pathogenesis, in particular the limitations of studying viral pathogenesis using animals lacking a key component of antiviral immunity. For instance, IFN-α/β-dependent restrictions on viral tropism or effects on B and T cell priming will not be evident in this model. Nonetheless, it is noteworthy that *Ifnar1*$^{-/-}$ mice sustained high levels of ZIKV infection in the brain, spinal cord, and testes. These tissues are relevant to aspects of ZIKV disease and epidemiology in humans including GBS, congenital infection/microcephaly, and sexual transmission. We detected ZIKV RNA in the brains and testes of *Ifnar1*$^{-/-}$ mice, even after disease signs had resolved. Although further studies are needed to characterize the nature of ZIKV persistent infection, these findings appear relevant to human infection, given that ZIKV RNA has been detected in semen up to 2 months after infection, from an otherwise healthy individual (Atkinson et al., 2016). Flaviviruses generally are not associated with persistent infection, but there is evidence of persistent WNV infection in the kidneys and long-term viral shedding in urine (Murray et al., 2010). In our studies, we infected mice with ZIKV via a subcutaneous route; this is a common method in flavivirus pathogenesis studies as it mimics key aspects of mosquito-transmitted infection including local replication at the inoculation site, spread to the draining lymph node, and establishment of viremia prior to hematogenous dissemination to distant sites. However, the public health urgency of the current ZIKV outbreak has been driven primarily by non-mosquito transmission routes, most notably congenital infection and sexual transmission. Although further experiments are needed to develop pathogenesis models that mimic these transmission routes, the present model in *Ifnar1*$^{-/-}$ mice is a valuable starting point. The presence of infectious ZIKV in the testes suggests a path forward for addressing key questions in the field including the duration of viral persistence over time, defining the component cells that support ZIKV infection in this immune privileged site, and developing mouse models of sexual transmission.

To create an even more useful animal model, infection studies are planned with more immunologically competent mice, including mice that conditionally lack IFN-α/β signaling on specific cell types, analogous to recent studies with DENV (Pinto et al., 2015). The development of viremia in MAR1-5A3-treated mice may be important for vaccine studies, as it allows for the induction of native adaptive immune responses in WT mice with subsequent attenuation of IFN-α/β responses and innate immunity prior to ZIKV challenge studies. Antibody blockade of IFN-α/β signaling with MAR1-5A3, however, did not recapitulate the severity of ZIKV disease phenotype observed in *Ifnar1*$^{-/-}$ mice, despite using high doses (2 mg or 133 mg/kg per 4-week-old mouse). Whereas all ZIKV-infected *Ifnar1*$^{-/-}$ mice showed evidence of neurological disease, MAR1-5A3-treated mice appeared healthy even though levels of ZIKV viremia were substantially higher than isotype control-treated mice at day 3 after infection, when it was tested. This result contrasts with prior studies with WNV, which showed that pre-treatment of WT mice with MAR-5A3 phenocopied *Ifnar1*$^{-/-}$ mice, with complete lethality observed (Pinto et al., 2011; Sheehan et al., 2015). The disparity between ZIKV and WNV phenotypes in *Ifnar1*$^{-/-}$- and MAR1-5A3-treated mice may reflect the mechanism of lethal disease. In WNV, death in *Ifnar1*$^{-/-}$- and MAR1-5A3-treated mice occurred rapidly (3–5 days post-infection) and was due to a MAVS-dependent virus-induced sepsis (Pinto

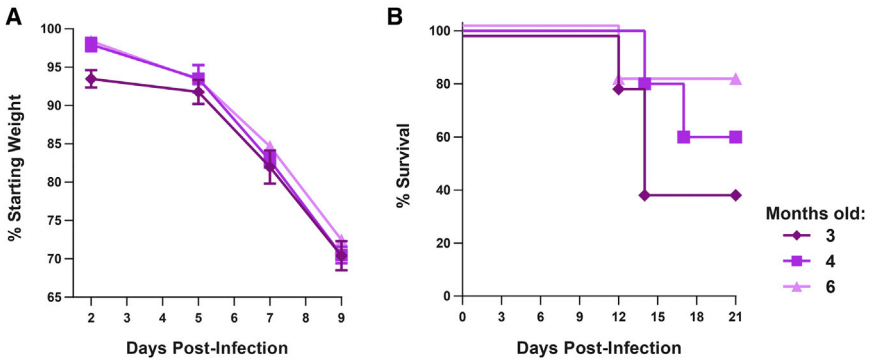

Figure 4. Older *Ifnar1*$^{-/-}$ Mice Remain Susceptible to ZIKV Infection

(A and B) Three-, four-, or six-month-old *Ifnar1*$^{-/-}$ C57BL/6 mice were infected with 10^3 FFU of ZIKV (H/PF/2013) by a subcutaneous route. (A) Mice were weighed over 21 days with data censored at 9 days after infection, when mice began to succumb. Weights are expressed as a percentage of starting weight, shown as the mean ± SEM of five mice per group. (B) Survival was monitored for 21 days.

et al., 2014). In contrast, ZIKV-induced death in *Ifnar1*$^{-/-}$ mice occurred later (8–12 days post-infection) and was associated with viral infection in the brain and spinal cord, as well as neurological signs including paralysis and encephalitis. MAR1-5A3 treatment may not enhance ZIKV infection and disease in the CNS because the antibody does not cross the blood-brain barrier efficiently and therefore has limited impact on IFN-α/β signaling in these tissues.

In summary, our results show that IFN-α/β signaling plays a key role in restricting ZIKV infection in mice. The use of mice with diminished or absent IFN-α/β signaling provides a small animal model for evaluating vaccines and therapeutics to combat ZIKV. Such models also will be valuable for studying the pathogenesis of ZIKV and mechanisms of viral immune evasion and for understanding unexpected clinical manifestations of ZIKV infection in humans.

EXPERIMENTAL PROCEDURES

Ethics Statement

This study was carried out in accordance with the recommendations in the Guide for the Care and Use of Laboratory Animals of the National Institutes of Health. The protocols were approved by the Institutional Animal Care and Use Committee at the Washington University School of Medicine (assurance no. A3381-01). Inoculations were performed under anesthesia that was induced and maintained with ketamine hydrochloride and xylazine, and all efforts were made to minimize animal suffering.

Cells

Vero cells (African green monkey kidney epithelial cells) were maintained in DMEM supplemented with 5% fetal bovine serum (Omega) and L-glutamine at 37°C with 5% CO_2. C6/36 *Aedes albopictus* cells were maintained in DMEM (4.5 g/L glucose, L-glutamine, and sodium pyruvate) supplemented with 10% fetal bovine serum (Hyclone), non-essential amino acids, and HEPES at 28°C with 5% CO_2.

Viruses

ZIKV strains MR 766 (Uganda, 1947), Dakar 41519 (Senegal, 1984), Dakar 41667 (Senegal, 1984), and Dakar 41671 (Senegal, 1984) were provided by the World Reference Center for Emerging Viruses and Arboviruses (R. Tesh, University of Texas Medical Branch) (Dick et al., 1952; Haddow et al., 2012; Kuno and Chang, 2007). ZIKV strain H/PF/2013 (French Polynesia, 2013) was provided by the Arbovirus Branch of the Centers for Disease Control and Prevention with permission (X. de Lamballerie, Aix Marseille Université) (Baronti et al., 2014). ZIKV stocks were propagated in C6/36 *Aedes albopictus* or Vero cells after inoculating at a multiplicity of infection of 0.01 and harvesting supernatants after 96 and 72 hr, respectively. Virus stocks were titrated by focus-forming assay (FFA) on Vero cells (Brien et al., 2013). Infected cell foci were detected at 48 hr after infection, following fixation with 1% paraformaldehyde and incubation with 500 ng/ml of flavivirus cross-reactive mouse monoclonal antibody E60 (Oliphant et al., 2006) for 2 hr at room temperature. After incubation for 1 hr with a 1:5,000 dilution of horseradish peroxidase (HRP)-conjugated goat anti-mouse IgG (Sigma), foci were detected by addition of TrueBlue substrate (KPL). Foci were analyzed with a CTL Immunospot instrument. Studies with ZIKV were conducted under biosafety level 2 (BSL2) and animal BSL3 (A-BSL3) containment at Washington University School of Medicine with Institutional Biosafety Committee approval.

Mouse Experiments

Transgenic mice analyzed included *Ifnar1*$^{-/-}$ (Daffis et al., 2011), *Irf3*$^{-/-}$ *Irf5*$^{-/-}$ *Irf7*$^{-/-}$ TKO (Lazear et al., 2013), *Mavs*$^{-/-}$ (Suthar et al., 2010), *Irf3*$^{-/-}$ (Sato et al., 2000), *Irf5*$^{-/-}$ (Takaoka et al., 2005), AG129 (van den Broek et al., 1995), *Ifnlr1*$^{-/-}$ (Ank et al., 2008), *Ifit1*$^{-/-}$ (Szretter et al., 2012), *Ifit2*$^{-/-}$ (Fensterl et al., 2012), *Ifitm3*$^{-/-}$ (Lange et al., 2008), *Isg15*$^{-/-}$ (Osiak et al., 2005), *Ube1l*$^{-/-}$ (Kim et al., 2006), *Mb21d*$^{-/-}$ (cGas) (Schoggins et al., 2014), and *Tmem173*$^{-/-}$ (STING) (Sauer et al., 2011). All mice were on a C57BL/6 background except

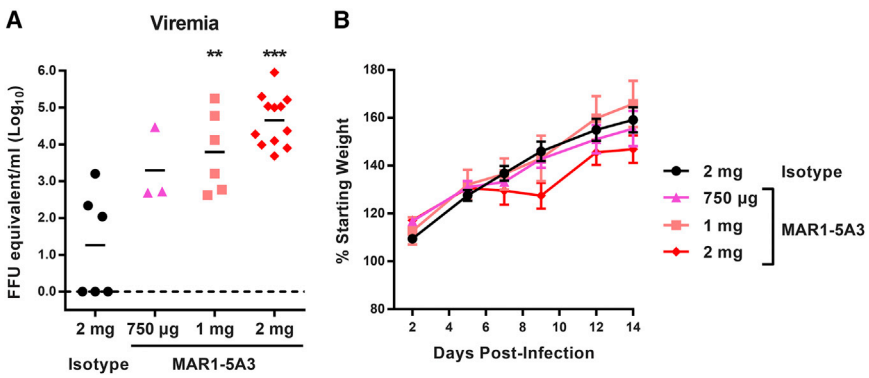

Figure 5. Treatment with an IFNAR1-Blocking mAb Increases ZIKV Viremia in WT Mice

(A and B) An IFNAR1-blocking mAb (MAR1-5A3) or isotype control mAb (GIR-208) was administered to 4- to 5-week-old WT C57BL/6 mice by i.p. injection. Mice were infected with 10^3 FFU of ZIKV (H/PF/2013) by a subcutaneous route. (A) ZIKV RNA in serum was measured at 3 days after infection by qRT-PCR. Data are expressed as FFU equivalents per milliliter after normalization to a standard curve generated in parallel. **$p < 0.01$; ***$p < 0.001$ compared to isotype control (Mann-Whitney test). (B) Weights are expressed as a percentage of starting weight, shown as the mean ± SEM of six mice per group.

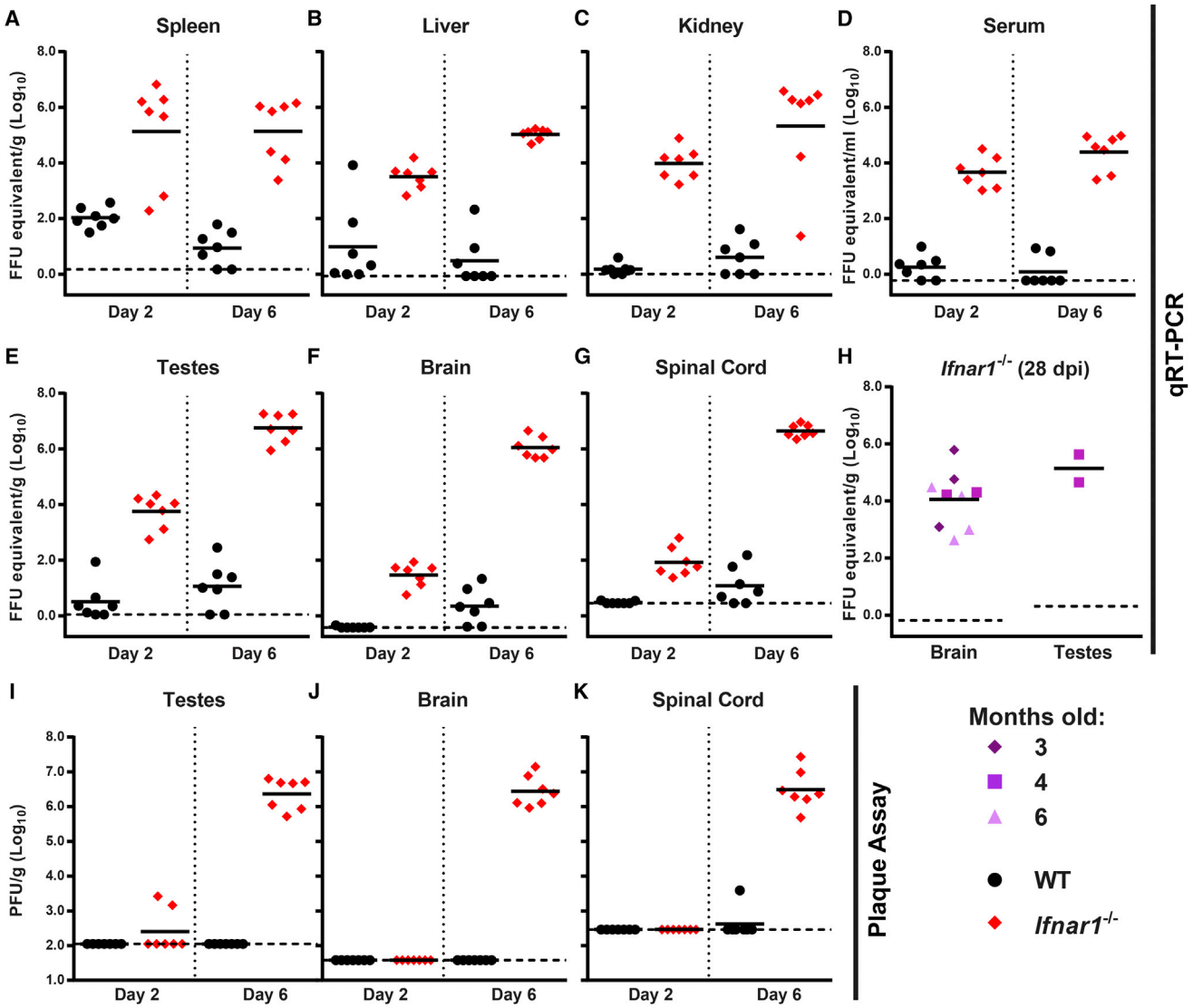

Figure 6. Tissue Tropism of ZIKV in WT and *Ifnar1*$^{-/-}$ Mice

(A–K) Four- to six-week-old WT or *Ifnar1*$^{-/-}$ C57BL/6 male mice were inoculated with 10^3 FFU of ZIKV H/PF/2013 by a subcutaneous route. At day 2 or day 6 after infection, the indicated tissues were harvested, weighed, homogenized, and analyzed by qRT-PCR (A–G) or plaque assay (I–K). Results are combined from two independent experiments with a total of seven mice per group; data are expressed as FFU equivalents per gram or milliliter after normalization to a standard curve generated in parallel (A–G) or as plaque-forming units (PFU) per gram (I–K). (H) Brain and testes were harvested 28 days after infection from 3-, 4-, or 6-month old *Ifnar1*$^{-/-}$ mice inoculated with 10^3 FFU of ZIKV H/PF/2013, and viral RNA levels were determined by qRT-PCR. These mice are the survivors from experiments shown in Figure 4 (all surviving mice for brain tissue, males only for testes).

for AG129 and CD-1. Mice were bred in a specific-pathogen-free facility at Washington University or purchased from Jackson Laboratories (WT C57BL/6 and CD-1). Mice were inoculated with ZIKV by subcutaneous (footpad), intravenous (retro-orbital), or i.p. routes with 10^2, 10^3, or 10^4 FFU of ZIKV in a volume of 50 μL. Survival, weight loss, and disease signs were monitored for 14–30 days, depending on the experiment. To evaluate clinical disease, mice were assigned to one of the following categories each day: (A) no disease, (B) hindlimb weakness or disrupted righting reflex, (C) partial hindlimb paralysis or toe knuckling, (D) complete paralysis of one hindlimb, (E) complete paralysis of both hindlimbs, (F) complete paralysis of all four limbs, or (G) moribund or dead; mice with a disease score of F or G were euthanized. In some experiments, WT mice were treated with indicated doses of an IFNAR-blocking mouse mAb (MAR1-5A3) or isotype control mouse mAb (GIR-208) (produced by Leinco Technologies) (Sheehan et al., 2006, 2015) by i.p. injection.

Measurement of Viral Burden

ZIKV-infected mice were euthanized at 2, 6, or 28 days after infection and perfused with 20 ml of PBS. Liver, spleen, kidney, testes, brain, and spinal cord were harvested, weighed, and homogenized with zirconia beads in a MagNA Lyser instrument (Roche Life Science) in 1 ml of minimal essential medium (MEM) supplemented with 2% heat-inactivated FBS. Blood was collected and allowed to clot at room temperature; serum was separated by centrifugation. All homogenized tissues and serum from infected animals were stored at −80°C until virus titration. With some samples, viral burden was determined by plaque assay on Vero cells. Samples were thawed, clarified by centrifugation (2,000× *g* at 4°C for 10 min), and then diluted serially prior to infection of Vero cells. Plaque assays were overlaid with agarose and 4 days later were fixed with 10% formaldehyde and stained with crystal violet (Brien et al., 2013). Tissue samples and serum from ZIKV-infected

mice were extracted with the RNeasy Mini Kit (tissues) or Viral RNA Mini Kit (serum) (QIAGEN). ZIKV RNA levels were determined by TaqMan one-step quantitative reverse transcriptase PCR (qRT-PCR) on an ABI 7500 Fast Instrument using standard cycling conditions. Viral burden is expressed on a $\log_{10}$ scale as viral RNA equivalents per gram or per milliliter after comparison with a standard curve produced using serial 10-fold dilutions of ZIKV RNA. A previously published primer set was used to detect ZIKV RNA (Lanciotti et al., 2008): forward, 5′-CCGCTGCCCAACACAAG-3′; reverse, 5′-CCACTAACGTTCTTTTGCAGACAT-3′; probe, 5′-/56-FAM/AGCCTACCT/ZEN/TGACAAGCAATCAGACACTCAA/3IABkFQ/-3′ (Integrated DNA Technologies).

Data Analysis

All data were analyzed with GraphPad Prism software. Kaplan-Meier survival curves were analyzed by the log rank test, and weight losses were compared using two-way ANOVA. For viral burden analysis, the log titers and levels of viral RNA were analyzed by the Mann-Whitney test. A p value of < 0.05 indicated statistically significant differences.

AUTHOR CONTRIBUTIONS

H.M.L., J.J.M., J.G., and M.S.D. designed experiments. H.M.L., J.G., J.J.M., A.M.S., E.F., and D.J.P. performed the experiments. H.M.L., J.G., J.J.M., and A.M.S. analyzed the data. H.M.L. and M.S.D. wrote the first draft of the paper; all authors edited the manuscript.

ACKNOWLEDGMENTS

This work was supported by start-up funds from the University of North Carolina Department of Microbiology and Immunology and the Lineberger Comprehensive Cancer Center (H.M.L.), as well as grants from the NIH (R01 AI073755 and R01 AI104972) (M.S.D.). J.J.M., E.F., and D.J.P. were supported by a Rheumatology Research Foundation Scientist Development Award, NIH Pre-Doctoral Training Grant award (T32 AI007163), and NIH Research Education Program (R25 HG006687), respectively. M.S.D. is a consultant for InBios and Visterra and a member of the Scientific Advisory Board of Moderna.

Received: March 18, 2016
Revised: March 28, 2016
Accepted: March 28, 2016
Published: April 5, 2016

REFERENCES

Alkan, C., Zapata, S., Bichaud, L., Moureau, G., Lemey, P., Firth, A.E., Gritsun, T.S., Gould, E.A., de Lamballerie, X., Depaquit, J., and Charrel, R.N. (2015). Ecuador Paraiso Escondido Virus, a New Flavivirus Isolated from New World Sand Flies in Ecuador, Is the First Representative of a Novel Clade in the Genus Flavivirus. J. Virol. *89*, 11773–11785.

Ank, N., Iversen, M.B., Bartholdy, C., Staeheli, P., Hartmann, R., Jensen, U.B., Dagnaes-Hansen, F., Thomsen, A.R., Chen, Z., Haugen, H., et al. (2008). An important role for type III interferon (IFN-lambda/IL-28) in TLR-induced antiviral activity. J. Immunol. *180*, 2474–2485.

Atkinson, B., Hearn, P., Afrough, B., Lumley, S., Carter, D., Aarons, E.J., Simpson, A.J., Brooks, T.J., and Hewson, R. (2016). Detection of Zika Virus in Semen. Emerg. Infect. Dis. *22*, http://dx.doi.org/10.3201/eid2205.160107.

Baronti, C., Piorkowski, G., Charrel, R.N., Boubis, L., Leparc-Goffart, I., and de Lamballerie, X. (2014). Complete coding sequence of zika virus from a French polynesia outbreak in 2013. Genome Announc. *2*, e00500–e00514.

Bell, T.M., Field, E.J., and Narang, H.K. (1971). Zika virus infection of the central nervous system of mice. Arch. Gesamte Virusforsch. *35*, 183–193.

Brasil, P., Pereira, J.P., Jr., Raja Gabaglia, C., Damasceno, L., Wakimoto, M., Ribeiro Nogueira, R.M., Carvalho de Sequeira, P., Machado Siqueira, A., Abreu de Carvalho, L.M., Cotrim da Cunha, D., et al. (2016). Zika Virus Infection in Pregnant Women in Rio de Janeiro - Preliminary Report. N. Engl. J. Med. Published online March 4, 2016. http://dx.doi.org/10.1056/NEJMoa1602412.

Brien, J.D., Lazear, H.M., and Diamond, M.S. (2013). Propagation, quantification, detection, and storage of West Nile virus. Curr. Protoc. Microbiol. *31*, 1, 18. http://dx.doi.org/10.1002/9780471729259.mc15d03s31.

Calvet, G., Aguiar, R.S., Melo, A.S., Sampaio, S.A., de Filippis, I., Fabri, A., Araujo, E.S., de Sequeira, P.C., de Mendonça, M.C., de Oliveira, L., et al. (2016). Detection and sequencing of Zika virus from amniotic fluid of fetuses with microcephaly in Brazil: a case study. Lancet Infect. Dis. Published online February 17, 2016. http://dx.doi.org/10.1016/S1473-3099(16)00095-5.

Cao-Lormeau, V.M., Roche, C., Teissier, A., Robin, E., Berry, A.L., Mallet, H.P., Sall, A.A., and Musso, D. (2014). Zika virus, French polynesia, South pacific, 2013. Emerg. Infect. Dis. *20*, 1085–1086.

Cao-Lormeau, V.M., Blake, A., Mons, S., Lastère, S., Roche, C., Vanhomwegen, J., Dub, T., Baudouin, L., Teissier, A., Larre, P., et al. (2016). Guillain-Barré Syndrome outbreak associated with Zika virus infection in French Polynesia: a case-control study. Lancet. Published online February 29, 2016. http://dx.doi.org/10.1016/S0140-6736(16)00562-6.

Cauchemez, S., Besnard, M., Bompard, P., Dub, T., Guillemette-Artur, P., Eyrolle-Guignot, D., Salje, H., Van Kerkhove, M.D., Abadie, V., Garel, C., et al. (2016). Association between Zika virus and microcephaly in French Polynesia, 2013-15: a retrospective study. Lancet. Published online March 15, 2016. http://dx.doi.org/10.1016/S0140-6736(16)00651-6.

Daffis, S., Lazear, H.M., Liu, W.J., Audsley, M., Engle, M., Khromykh, A.A., and Diamond, M.S. (2011). The naturally attenuated Kunjin strain of West Nile virus shows enhanced sensitivity to the host type I interferon response. J. Virol. *85*, 5664–5668.

de Paula Freitas, B., de Oliveira Dias, J.R., Prazeres, J., Sacramento, G.A., Ko, A.I., Maia, M., and Belfort, R., Jr. (2016). Ocular Findings in Infants With Microcephaly Associated With Presumed Zika Virus Congenital Infection in Salvador, Brazil. JAMA Ophthalmol. http://dx.doi.org/10.1001/jamaophthalmol.2016.0267.

Dick, G.W. (1952). Zika virus. II. Pathogenicity and physical properties. Trans. R. Soc. Trop. Med. Hyg. *46*, 521–534.

Dick, G.W., Kitchen, S.F., and Haddow, A.J. (1952). Zika virus. I. Isolations and serological specificity. Trans. R. Soc. Trop. Med. Hyg. *46*, 509–520.

Duffy, M.R., Chen, T.H., Hancock, W.T., Powers, A.M., Kool, J.L., Lanciotti, R.S., Pretrick, M., Marfel, M., Holzbauer, S., Dubray, C., et al. (2009). Zika virus outbreak on Yap Island, Federated States of Micronesia. N. Engl. J. Med. *360*, 2536–2543.

European Centre for Disease Prevention and Control (2016). Zika virus disease epidemic: potential association with microcephaly and Guillain-Barré syndrome (first update) (Stockholm: ECDC).

Fensterl, V., Wetzel, J.L., Ramachandran, S., Ogino, T., Stohlman, S.A., Bergmann, C.C., Diamond, M.S., Virgin, H.W., and Sen, G.C. (2012). Interferon-induced Ifit2/ISG54 protects mice from lethal VSV neuropathogenesis. PLoS Pathog. *8*, e1002712.

Foy, B.D., Kobylinski, K.C., Chilson Foy, J.L., Blitvich, B.J., Travassos da Rosa, A., Haddow, A.D., Lanciotti, R.S., and Tesh, R.B. (2011). Probable non-vector-borne transmission of Zika virus, Colorado, USA. Emerg. Infect. Dis. *17*, 880–882.

Haddow, A.J., Williams, M.C., Woodall, J.P., Simpson, D.I., and Goma, L.K. (1964). Twelve Isolations of Zika Virus from Aedes (Stegomyia) Africanus (Theobald) Taken in and above a Uganda Forest. Bull. World Health Organ. *31*, 57–69.

Haddow, A.D., Schuh, A.J., Yasuda, C.Y., Kasper, M.R., Heang, V., Huy, R., Guzman, H., Tesh, R.B., and Weaver, S.C. (2012). Genetic characterization of Zika virus strains: geographic expansion of the Asian lineage. PLoS Negl. Trop. Dis. *6*, e1477.

Hamel, R., Dejarnac, O., Wichit, S., Ekchariyawat, P., Neyret, A., Luplertlop, N., Perera-Lecoin, M., Surasombatpattana, P., Talignani, L., Thomas, F., et al. (2015). Biology of Zika Virus Infection in Human Skin Cells. J. Virol. *89*, 8880–8896.

Hayes, E.B. (2009). Zika virus outside Africa. Emerg. Infect. Dis. *15*, 1347–1350.

Hills, S.L., Russell, K., Hennessey, M., Williams, C., Oster, A.M., Fischer, M., and Mead, P. (2016). Transmission of Zika Virus Through Sexual Contact with Travelers to Areas of Ongoing Transmission - Continental United States, 2016. MMWR Morb. Mortal. Wkly. Rep. *65*, 215–216.

Johnson, B.K., Chanas, A.C., Shockley, P., Squires, E.J., Gardner, P., Wallace, C., Simpson, D.I., Bowen, E.T., Platt, G.S., Way, H., et al. (1977). Arbovirus isolations from, and serological studies on, wild and domestic vertebrates from Kano Plain, Kenya. Trans. R. Soc. Trop. Med. Hyg. *71*, 512–517.

Kim, K.I., Yan, M., Malakhova, O., Luo, J.K., Shen, M.F., Zou, W., de la Torre, J.C., and Zhang, D.E. (2006). Ube1L and protein ISGylation are not essential for alpha/beta interferon signaling. Mol. Cell. Biol. *26*, 472–479.

Kuno, G., and Chang, G.J. (2007). Full-length sequencing and genomic characterization of Bagaza, Kedougou, and Zika viruses. Arch. Virol. *152*, 687–696.

Lanciotti, R.S., Kosoy, O.L., Laven, J.J., Velez, J.O., Lambert, A.J., Johnson, A.J., Stanfield, S.M., and Duffy, M.R. (2008). Genetic and serologic properties of Zika virus associated with an epidemic, Yap State, Micronesia, 2007. Emerg. Infect. Dis. *14*, 1232–1239.

Lange, U.C., Adams, D.J., Lee, C., Barton, S., Schneider, R., Bradley, A., and Surani, M.A. (2008). Normal germ line establishment in mice carrying a deletion of the Ifitm/Fragilis gene family cluster. Mol. Cell. Biol. *28*, 4688–4696.

Lazear, H.M., and Diamond, M.S. (2016). Zika Virus: New Clinical Syndromes and its Emergence in the Western Hemisphere. J. Virol. Published online March 9, 2016. http://dx.doi.org/10.1128/JVI.00252-16.

Lazear, H.M., Lancaster, A., Wilkins, C., Suthar, M.S., Huang, A., Vick, S.C., Clepper, L., Thackray, L., Brassil, M.M., Virgin, H.W., et al. (2013). IRF-3, IRF-5, and IRF-7 coordinately regulate the type I IFN response in myeloid dendritic cells downstream of MAVS signaling. PLoS Pathog. *9*, e1003118.

Lim, P.Y., Behr, M.J., Chadwick, C.M., Shi, P.Y., and Bernard, K.A. (2011). Keratinocytes are cell targets of West Nile virus in vivo. J. Virol. *85*, 5197–5201.

Limon-Flores, A.Y., Perez-Tapia, M., Estrada-Garcia, I., Vaughan, G., Escobar-Gutierrez, A., Calderon-Amador, J., Herrera-Rodriguez, S.E., Brizuela-Garcia, A., Heras-Chavarria, M., Flores-Langarica, A., et al. (2005). Dengue virus inoculation to human skin explants: an effective approach to assess in situ the early infection and the effects on cutaneous dendritic cells. Int. J. Exp. Pathol. *86*, 323–334.

Martines, R.B., Bhatnagar, J., Keating, M.K., Silva-Flannery, L., Muehlenbachs, A., Gary, J., Goldsmith, C., Hale, G., Ritter, J., Rollin, D., et al. (2016). Notes from the Field: Evidence of Zika Virus Infection in Brain and Placental Tissues from Two Congenitally Infected Newborns and Two Fetal Losses - Brazil, 2015. MMWR Morb. Mortal. Wkly. Rep. *65*, 159–160.

McCrae, A.W., and Kirya, B.G. (1982). Yellow fever and Zika virus epizootics and enzootics in Uganda. Trans. R. Soc. Trop. Med. Hyg. *76*, 552–562.

Meier, K.C., Gardner, C.L., Khoretonenko, M.V., Klimstra, W.B., and Ryman, K.D. (2009). A mouse model for studying viscerotropic disease caused by yellow fever virus infection. PLoS Pathog. *5*, e1000614.

Mlakar, J., Korva, M., Tul, N., Popović, M., Poljšak-Prijatelj, M., Mraz, J., Kolenc, M., Resman Rus, K., Vesnaver Vipotnik, T., Fabjan Vodušek, V., et al. (2016). Zika Virus Associated with Microcephaly. N. Engl. J. Med. *374*, 951–958.

Murray, K., Walker, C., Herrington, E., Lewis, J.A., McCormick, J., Beasley, D.W., Tesh, R.B., and Fisher-Hoch, S. (2010). Persistent infection with West Nile virus years after initial infection. J. Infect. Dis. *201*, 2–4.

Musso, D., Roche, C., Robin, E., Nhan, T., Teissier, A., and Cao-Lormeau, V.M. (2015). Potential sexual transmission of Zika virus. Emerg. Infect. Dis. *21*, 359–361.

Oehler, E., Watrin, L., Larre, P., Leparc-Goffart, I., Lastere, S., Valour, F., Baudouin, L., Mallet, H., Musso, D., and Ghawche, F. (2014). Zika virus infection complicated by Guillain-Barre syndrome–case report, French Polynesia, December 2013. Euro Surveill. *19*, 20720.

Oliphant, T., Nybakken, G.E., Engle, M., Xu, Q., Nelson, C.A., Sukupolvi-Petty, S., Marri, A., Lachmi, B.E., Olshevsky, U., Fremont, D.H., et al. (2006). Antibody recognition and neutralization determinants on domains I and II of West Nile Virus envelope protein. J. Virol. *80*, 12149–12159.

Oliveira Melo, A.S., Malinger, G., Ximenes, R., Szejnfeld, P.O., Alves Sampaio, S., and Bispo de Filippis, A.M. (2016). Zika virus intrauterine infection causes fetal brain abnormality and microcephaly: tip of the iceberg? Ultrasound Obstet. Gynecol. *47*, 6–7, http://dx.doi.org/10.1002/uog.15831.

Osiak, A., Utermöhlen, O., Niendorf, S., Horak, I., and Knobeloch, K.P. (2005). ISG15, an interferon-stimulated ubiquitin-like protein, is not essential for STAT1 signaling and responses against vesicular stomatitis and lymphocytic choriomeningitis virus. Mol. Cell. Biol. *25*, 6338–6345.

Pagni, S., and Fernandez-Sesma, A. (2012). Evasion of the human innate immune system by dengue virus. Immunol. Res. *54*, 152–159.

Petersen, E.E., Staples, J.E., Meaney-Delman, D., Fischer, M., Ellington, S.R., Callaghan, W.M., and Jamieson, D.J. (2016). Interim Guidelines for Pregnant Women During a Zika Virus Outbreak - United States, 2016. MMWR Morb. Mortal. Wkly. Rep. *65*, 30–33.

Pierson, T.C., and Diamond, M.S. (2013). Flaviviruses. In Fields Virology, D.M. Knipe and P.M. Howley, eds. (Wolter Kluwer), pp. 747–794.

Pinto, A.K., Daffis, S., Brien, J.D., Gainey, M.D., Yokoyama, W.M., Sheehan, K.C., Murphy, K.M., Schreiber, R.D., and Diamond, M.S. (2011). A temporal role of type I interferon signaling in CD8+ T cell maturation during acute West Nile virus infection. PLoS Pathog. *7*, e1002407.

Pinto, A.K., Ramos, H.J., Wu, X., Aggarwal, S., Shrestha, B., Gorman, M., Kim, K.Y., Suthar, M.S., Atkinson, J.P., Gale, M., Jr., and Diamond, M.S. (2014). Deficient IFN signaling by myeloid cells leads to MAVS-dependent virus-induced sepsis. PLoS Pathog. *10*, e1004086.

Pinto, A.K., Brien, J.D., Lam, C.Y., Johnson, S., Chiang, C., Hiscott, J., Sarathy, V.V., Barrett, A.D., Shresta, S., and Diamond, M.S. (2015). Defining New Therapeutics Using a More Immunocompetent Mouse Model of Antibody-Enhanced Dengue Virus Infection. MBio *6*, e01316–e15.

Sarathy, V.V., Milligan, G.N., Bourne, N., and Barrett, A.D. (2015). Mouse models of dengue virus infection for vaccine testing. Vaccine *33*, 7051–7060.

Sarno, M., Sacramento, G.A., Khouri, R., do Rosário, M.S., Costa, F., Archanjo, G., Santos, L.A., Nery, N., Jr., Vasilakis, N., Ko, A.I., and de Almeida, A.R. (2016). Zika Virus Infection and Stillbirths: A Case of Hydrops Fetalis, Hydranencephaly and Fetal Demise. PLoS Negl. Trop. Dis. *10*, e0004517.

Sato, M., Suemori, H., Hata, N., Asagiri, M., Ogasawara, K., Nakao, K., Nakaya, T., Katsuki, M., Noguchi, S., Tanaka, N., and Taniguchi, T. (2000). Distinct and essential roles of transcription factors IRF-3 and IRF-7 in response to viruses for IFN-alpha/beta gene induction. Immunity *13*, 539–548.

Sauer, J.D., Sotelo-Troha, K., von Moltke, J., Monroe, K.M., Rae, C.S., Brubaker, S.W., Hyodo, M., Hayakawa, Y., Woodward, J.J., Portnoy, D.A., and Vance, R.E. (2011). The N-ethyl-N-nitrosourea-induced Goldenticket mouse mutant reveals an essential function of Sting in the in vivo interferon response to Listeria monocytogenes and cyclic dinucleotides. Infect. Immun. *79*, 688–694.

Schoggins, J.W., MacDuff, D.A., Imanaka, N., Gainey, M.D., Shrestha, B., Eitson, J.L., Mar, K.B., Richardson, R.B., Ratushny, A.V., Litvak, V., et al. (2014). Pan-viral specificity of IFN-induced genes reveals new roles for cGAS in innate immunity. Nature *505*, 691–695.

Sheehan, K.C., Lai, K.S., Dunn, G.P., Bruce, A.T., Diamond, M.S., Heutel, J.D., Dungo-Arthur, C., Carrero, J.A., White, J.M., Hertzog, P.J., and Schreiber, R.D. (2006). Blocking monoclonal antibodies specific for mouse IFN-alpha/beta receptor subunit 1 (IFNAR-1) from mice immunized by in vivo hydrodynamic transfection. J. Interferon Cytokine Res. *26*, 804–819.

Sheehan, K.C., Lazear, H.M., Diamond, M.S., and Schreiber, R.D. (2015). Selective Blockade of Interferon-α and -β Reveals Their Non-Redundant Functions in a Mouse Model of West Nile Virus Infection. PLoS ONE *10*, e0128636.

Surasombatpattana, P., Hamel, R., Patramool, S., Luplertlop, N., Thomas, F., Desprès, P., Briant, L., Yssel, H., and Missé, D. (2011). Dengue virus replication in infected human keratinocytes leads to activation of antiviral innate immune responses. Infect. Genet. Evol. *11*, 1664–1673.

Suthar, M.S., Ma, D.Y., Thomas, S., Lund, J.M., Zhang, N., Daffis, S., Rudensky, A.Y., Bevan, M.J., Clark, E.A., Kaja, M.K., et al. (2010). IPS-1 is essential for the control of West Nile virus infection and immunity. PLoS Pathog. *6*, e1000757.

Suthar, M.S., Aguirre, S., and Fernandez-Sesma, A. (2013). Innate immune sensing of flaviviruses. PLoS Pathog. *9*, e1003541.

Szretter, K.J., Daniels, B.P., Cho, H., Gainey, M.D., Yokoyama, W.M., Gale, M., Jr., Virgin, H.W., Klein, R.S., Sen, G.C., and Diamond, M.S. (2012). 2′-O methylation of the viral mRNA cap by West Nile virus evades ifit1-dependent and -independent mechanisms of host restriction in vivo. PLoS Pathog. *8*, e1002698.

Takaoka, A., Yanai, H., Kondo, S., Duncan, G., Negishi, H., Mizutani, T., Kano, S., Honda, K., Ohba, Y., Mak, T.W., and Taniguchi, T. (2005). Integral role of IRF-5 in the gene induction programme activated by Toll-like receptors. Nature *434*, 243–249.

Tang, H., Hammack, C., Ogden, S.C., Wen, Z., Qian, X., Li, Y., Yao, B., Shin, J., Zhang, F., Lee, E.M., et al. (2016). Zika Virus Infects Human Cortical Neural Progenitors and Attenuates Their Growth. Cell Stem Cell. Published online March 3, 2016. http://dx.doi.org/10.1016/j.stem.2016.02.016.

van den Broek, M.F., Müller, U., Huang, S., Aguet, M., and Zinkernagel, R.M. (1995). Antiviral defense in mice lacking both alpha/beta and gamma interferon receptors. J. Virol. *69*, 4792–4796.

Ventura, C.V., Maia, M., Bravo-Filho, V., Góis, A.L., and Belfort, R., Jr. (2016). Zika virus in Brazil and macular atrophy in a child with microcephaly. Lancet *387*, 228.

Venturi, G., Zammarchi, L., Fortuna, C., Remoli, M.E., Benedetti, E., Fiorentini, C., Trotta, M., Rizzo, C., Mantella, A., Rezza, G., and Bartoloni, A. (2016). An autochthonous case of Zika due to possible sexual transmission, Florence, Italy, 2014. Euro Surveill. *21*, http://dx.doi.org/10.2807/1560-7917.ES.2016.21.8.30148.

Way, J.H., Bowen, E.T., and Platt, G.S. (1976). Comparative studies of some African arboviruses in cell culture and in mice. J. Gen. Virol. *30*, 123–130.

Willison, H.J., Jacobs, B.C., and van Doorn, P.A. (2016). Guillain-Barré syndrome. Lancet. Published online February 29, 2016. http://dx.doi.org/10.1016/S0140-6736(16)00339-1.

Zellweger, R.M., Tang, W.W., Eddy, W.E., King, K., Sanchez, M.C., and Shresta, S. (2015). CD8+ T Cells Can Mediate Short-Term Protection against Heterotypic Dengue Virus Reinfection in Mice. J. Virol. *89*, 6494–6505.

Note Added in Proof

After acceptance, another paper was published confirming the utility of IFNAR1-deficient mice in the study of Zika virus pathogenesis: Rossi, S.L., Tesh, R.B., Azar, S.R., Muruato, A.E., Hanley, K.A., Auguste, A.J., Langsjoen, R.M., Paessler, S., Vasilakis, N., and Weaver, S.C. (2016). Characterization of a Novel Murine Model to Study Zika Virus. Am. J. Trop. Med. Hyg. Published online March 28, 2016. http://dx.doi.org/10.4269/ajtmh.16-0111.